Supporting Information

Improved Eco-Friendly Photovoltaics Based on Stabilized $AgBiS_2$ Nanocrystal Inks

Sung Yong Bae,[a,b] Jae Taek Oh,[b] Jin Young Park,[c] Su Ryong Ha,[b] Jongmin Choi,[c] Hyosung Choi[b,] and Younghoon Kim[a,]**

[a]Division of Energy Technology, Daegu Gyeongbuk Institute of Science and Technology (DGIST), 333 Techno Jungang-daero, Hyeonpung-myeon, Dalseong-gun, Daegu 42988, Republic of Korea

[b]Department of Chemistry and Research Institute for Convergence of Basic Sciences, Hanyang University, 222 Wangsimni-ro, Seongdong-gu, Seoul 04763, Republic of Korea

[c]Department of Energy Science and Engineering, Daegu Gyeongbuk Institute of Science and Technology (DGIST), 333 Techno Jungang-daero, Hyeonpung-myeon, Dalseong-gun, Daegu 42988, Republic of Korea

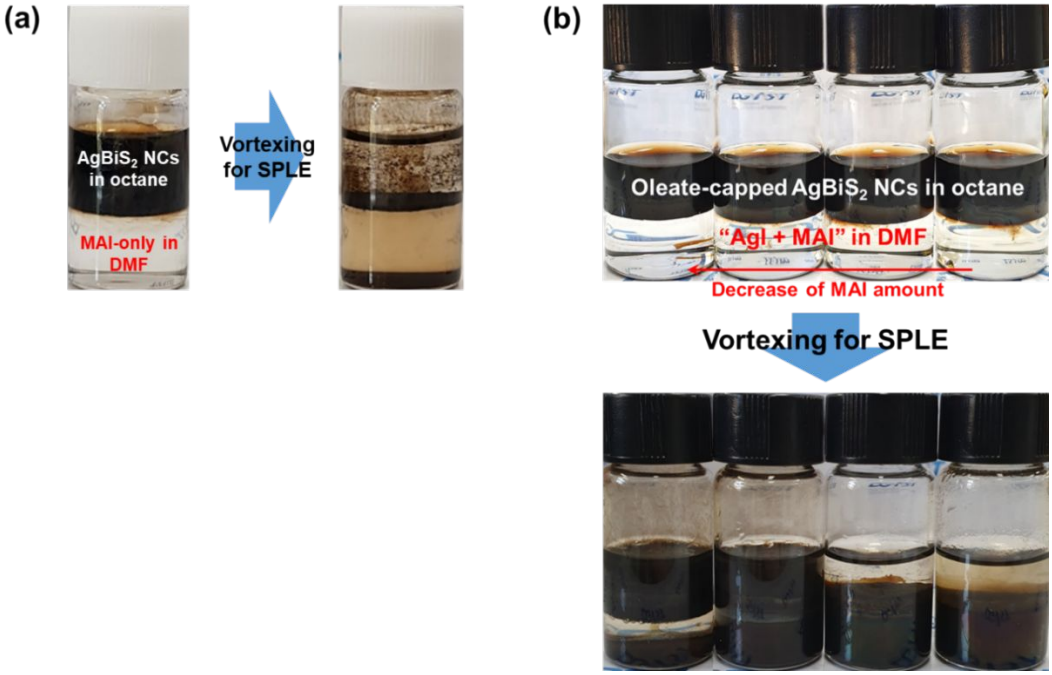

Figure S1. (a) Photo images of $AgBiS_2$ NCs before and after SPLE process using MAI-only DMF solution. (b) Photo images of $AgBiS_2$ NCs before and after SPLE process using AgI and MAI mixtures with different molar ratios in DMF (AgI:MAI = 1:0.2, 1:0.6, 1:0.8, 1:1).

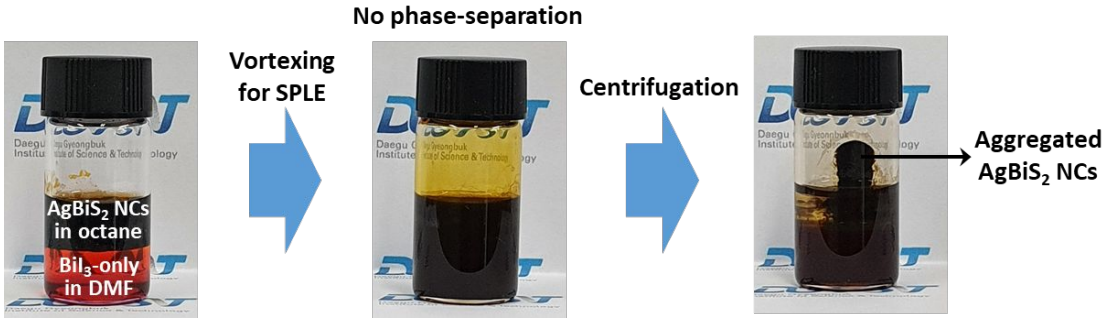

Figure S2. Photographs of the $AgBiS_2$ NCs before and after performing SPLE using a DMF solution of BiI_3 ligand only and in the absence of MAI.

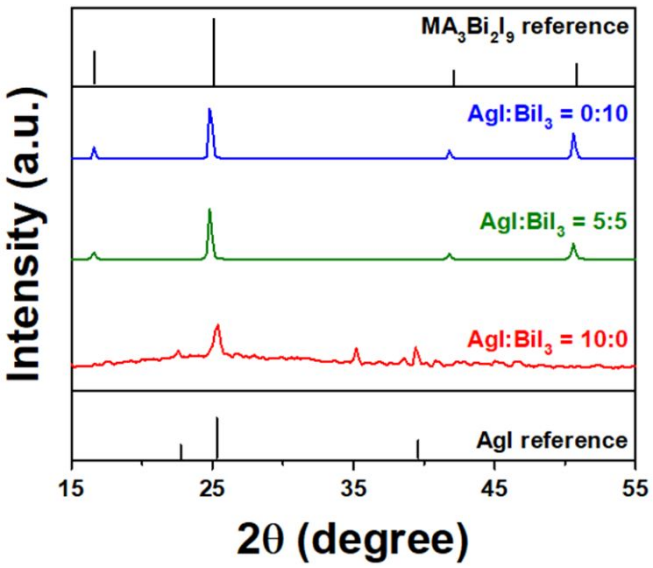

Figure S3. Thin film XRD spectra of the resultant films, spin-coated the halometallate ligand solutions with the molar ratios of AgI:BiI_3 to 10:0, 5:5 and 0:10 onto glass substrates and additionally annealed at 150 °C for 10 min under N_2-filled glove box. The reference XRD patterns for $MA_3Bi_2I_9$ and AgI were obtained from PDF Card No. 01-084-8254 and No. 01-078-0641, respectively.

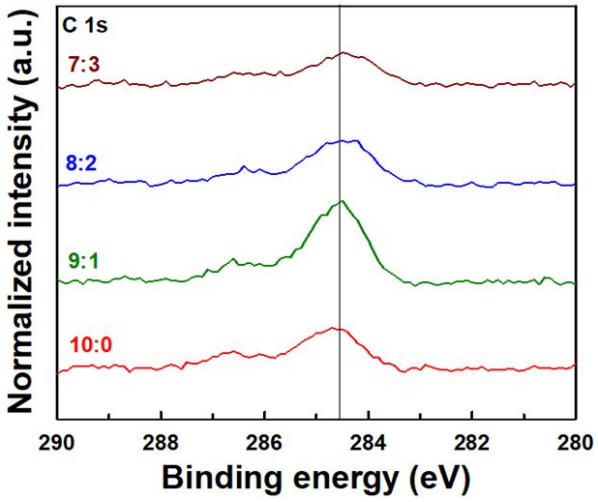

Figure S4. Normalized XPS C1s spectra of SPLE-induced $AgBiS_2$ NC solids using the different molar ratios of AgI to BiI_3.

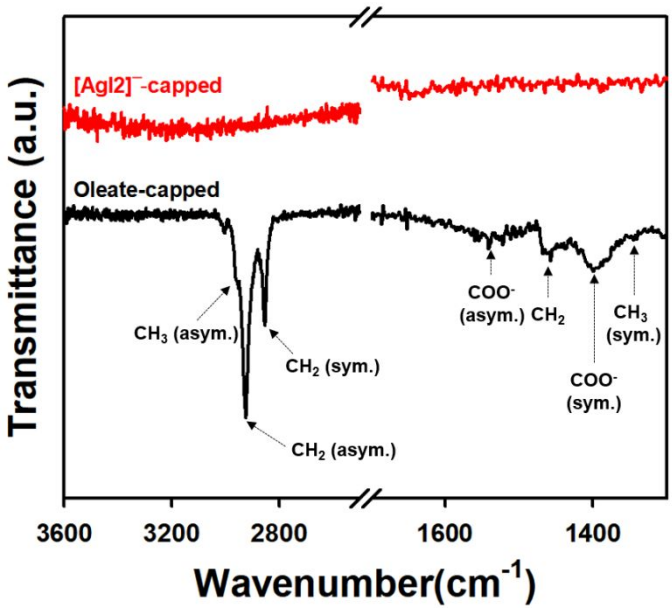

Figure S5. FT-IR spectra of the oleate-capped $AgBiS_2$ NCs before and after performing the SPLE process using a 10:0 ($AgI:BiI_3$) solution. The intensities of the peaks attributed to the C–H (2940, 2920, 2850 and 1450 cm^{-1}) and COO^- bonds (1580, 1380 cm^{-1}) significantly decreased in the spectrum of the $[AgI_2]^-$-capped $AgBiS_2$ NCs because of the successful replacement of long-chain oleate ligands with short-chain $[AgI_2]^-$ ions.

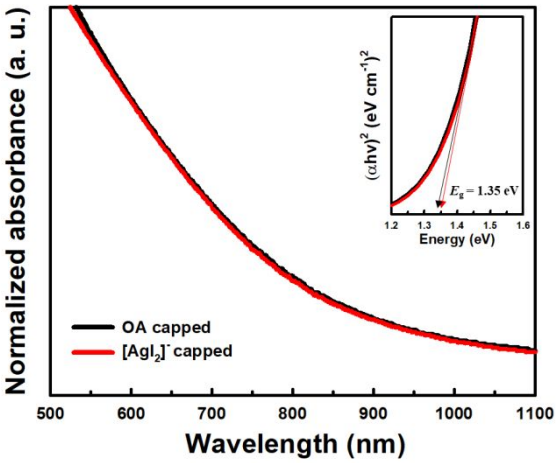

Figure S6. Absorbance spectra of as-cast and SPLE-prepared $AgBiS_2$ NCs using AgI-based halometallates. Inset graph shows the Tauc plots of each $AgBiS_2$ NC.

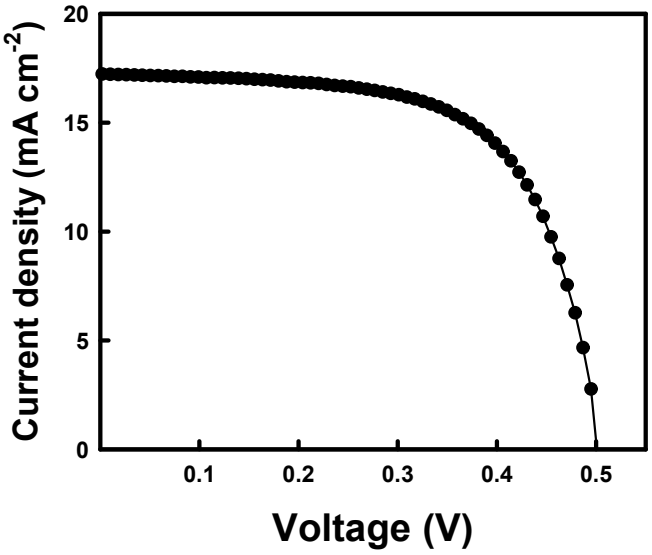

Figure S7. The *J–V* Curve of $AgBiS_2$ NC solar cell composed of SSLE-prepared $AgBiS_2$ NCs using TMAI ligand solutions.

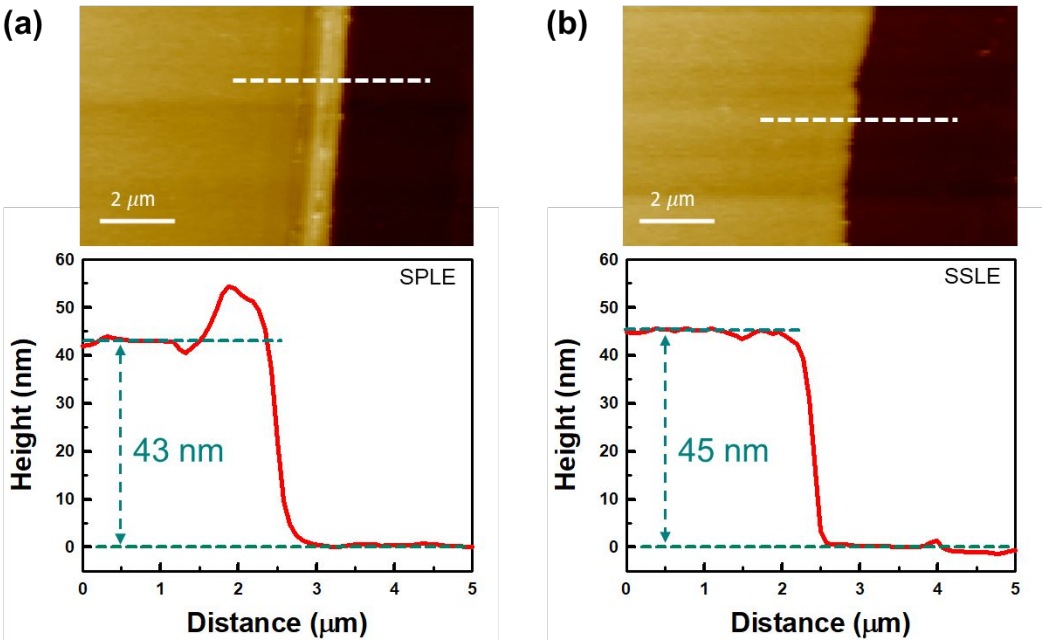

Figure S8. AFM images of (a) SPLE-prepared and (b) SSLE-prepared $AgBiS_2$ NC solids. The hegiht profiles of each solid are measured along the marked white lines and indicates the film thickness.

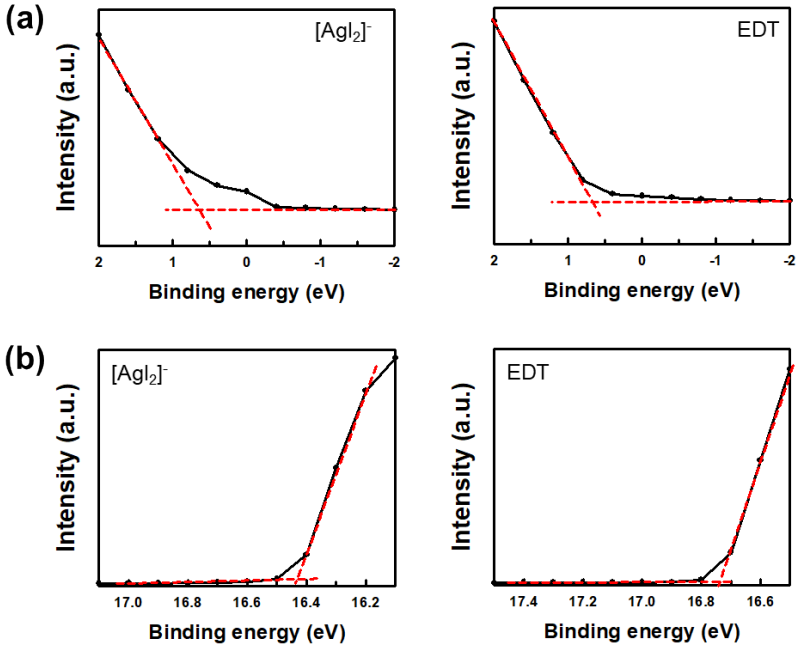

Figure S9. UPS spectra of SPLE-prepared $AgBiS_2$ NCs using AgI-based halometallates and SSLE-prepared $AgBiS_2$ NCs using EDT in (a) low binding-energy region and (b) high binding-energy region.

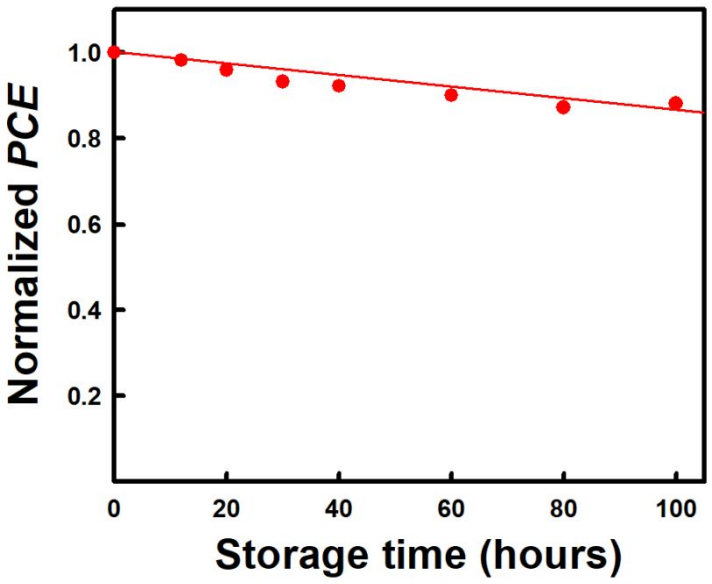

Figure S10. Device stability of the $AgBiS_2$ NC solar cell containing EDT-exchanged $AgBiS_2$ NC solids stored under dark ambient conditions.

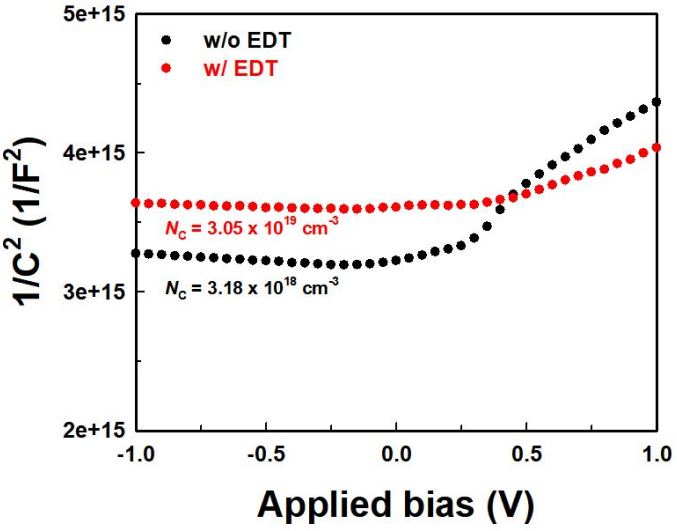

Figure S11. Mott-Schottky plots for the calculation of the carrier density of $AgBiS_2$ NCs prepared using AgI-based halometallates with and without EDT-exchanged $AgBiS_2$ NCs. The carrier density values were obtained from the Mott-Schottky plot following equation. (A is area, 0.09 cm^2)

$$\frac{1}{C^2} = \frac{2(\mathrm{Vbi} - V)}{A^2 e\, \varepsilon_{AgBiS_2} \varepsilon_0 N_{AgBiS_2}}$$

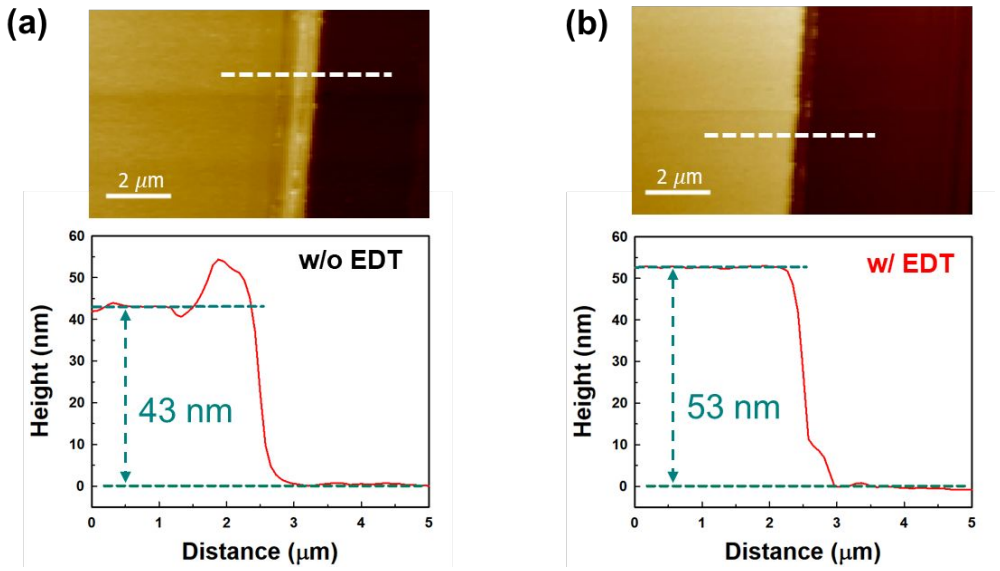

Figure S12. AFM images of the $[AgI_2]^-$-capped $AgBiS_2$ NC solids (a) without and (b) with EDT-exchanged $AgBiS_2$ NC solid. The hegiht profiles of each solid are measured along the marked white lines and indicates the film thickness.

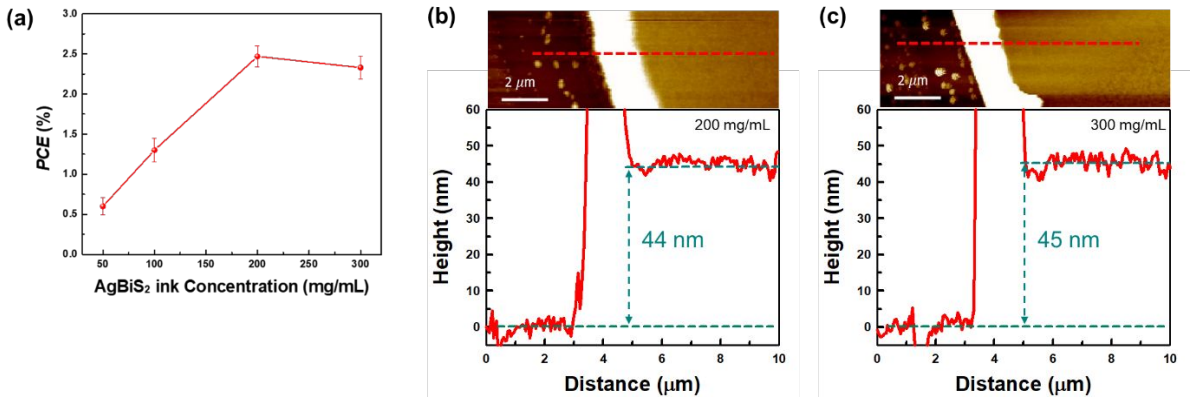

Figure S13. (a) Device performance of the $AgBiS_2$ NC solar cells based on various $[AgI_2]^-$-capped $AgBiS_2$ NC solids prepared using different ink concentrations. The AFM images of the $[AgI_2]^-$-capped $AgBiS_2$ NC solids prepared using NC concentrations of (b) 200 mg mL^{-1} and (c) 300 mg mL^{-1}. The height profile of each solid (measured along the marked white lines) indicates the film thickness.

Table S1. Photovoltaic parameters of the $AgBiS_2$ NC solar cells based on $[AgI_2]^-$-capped $AgBiS_2$ NC solids prepared using different ink concentrations.

$[AgI_2]^-$-capped $AgBiS_2$ NC Ink concentration (mg mL^{-1})	V_{OC} (V)	J_{SC} (mA cm^{-2})	*FF*	*PCE* (%)
50	0.25	6.19	0.38	0.60
100	0.32	10.01	0.41	1.30
200	0.47	11.88	0.45	2.47
300	0.49	8.96	0.53	2.33